Tiling-decoration model of the quasicrystal i-$Al_{73}Mn_{21}Si_6$

M. Mihalkovič and P. Mrafko
Institute of Physics, Slovak Academy of Sciences, CS-842 28 Bratislava, Slovakia
(Received 20 October 1992; revised manuscript received 28 June 1993)

We propose a tiling-and-decoration model of the icosahedral phase of Al-Mn-Si, in which a 126-atom "double" Mackay icosahedron and a 54-atom "simple" Mackay icosahedron alternate on the even and odd nodes of the tiling of four canonical cells. The model structure exhibits weak six-dimensional fcc ordering introduced by Al-vacancy alternation, similar to that observed in the related α phase. The density of the model is consistent with experimental data and calculation of the x-ray- and neutron-diffraction intensities leads to good agreement with experimental data in both cases: R factors are 0.09 and 0.16, respectively.

I. INTRODUCTION

The so-called tiling-and-decoration approach to the structure of quasicrystals is based on the assumption that a small number of favorable building blocks can be associated with the nodes, bonds, faces, and cells of the tiling, quasiperiodically filling the space. In the particular case of icosahedral quasicrystals, the favorable blocks are undoubtedly large icosahedral clusters, containing typically not less than 100 atoms. The structure of these clusters is well known—in Frank-Kasper (FK) phases they often order periodically on the bcc lattice, let us mention only two representative cases: α-Al-Mn-Si (Refs. 1 and 2) and α-Al-Zn-Mg.[3]

In spite of some interesting results,[4] the tiling-decoration scheme applied to the familiar three-dimensional (3D) Penrose tiling (3DPT) has led to difficulties that cannot be easily solved. The icosahedral clusters are in FK phases linked exclusively along twofold and threefold icosahedral directions, but there is no simple algorithm to find a good (dense) network based on the intercluster bonds that would uniquely decorate rhombohedra in the 3DPT. The experimental data were better reproduced by the models (for i-Al-Mn-Si, see Refs. 5–8) that treat icosahedral quasicrystals as six-dimensional cubic crystals. The real-space structure is obtained as an intersection of the properly oriented (with respect to the underlying 6D lattice) 3D "physical" space with 3D "atomic surfaces" decorating the 6D hypercubic lattice. The surfaces are embedded in complementary perpendicular $3D$ space.[9] The constraint on the boundaries of the atomic surfaces comes from such requirements as (i) avoiding unreasonably short real-space interatomic distances, (ii) faceting of the surfaces with the rational 6D planes, and (iii) mutual "closeness" of the surfaces in 6D.[10,11]

However, even if the 6D model is designed so as to maximize the density of the icosahedral clusters,[7] the above conditions constrain mostly the ordering of "connective" atoms, not belonging to the clusters, while there is still considerable freedom in the choice of clusters network. In fact, the requirement of maximal density of the icosahedral quasiperiodic networks—and this argument comes into play on both the atomic and cluster levels—is another physical constraint limiting the degrees of freedom in modeling, but the density of the available icosahedral quasiperiodic packings is obviously not maximal and no efficient density-maximization method is available.[12,13]

The model of the icosahedral phase Al-Mn-Si presented in this study (the preliminary short version was published in Ref. 14) is motivated by the recent proposal of the 3D icosahedral tiling,[15] which appears to be a promising alternative to the 3DPT as a basis for the models of icosahedral quasicrystals. Henley's tiling of four canonical cells (TCC) is based exclusively on the twofold and threefold intercluster bonds and it supports a straightforward implementation of the cluster-based decoration. In such a quasicrystal model, the long-range icosahedral order is promoted by the icosahedral clusters, while the "connective" atoms are rigidly filling a small number of allowed interstitials. The most important features of this model are the following: (i) The density of icosahedral clusters is supported to be maximal, (ii) the network of cluster centers is a tiling, and (iii) the fraction of the atoms, not belonging to the clusters is minimal. Fortunately, property (i) induces a *tractable* solution (ii): two bonds, three faces, and four tiles of the "tiling of canonical cells" (TCC).[15]

Another important ingredient of the model presented here are the "third" shells of the icosahedral clusters, found by Fowler *et al.*[16] and independently by Yang[17] in the α-Al-Mn-Si phase of the quasicrystal i-Al-Mn-Si. Seventy-two third-shell atoms occupy vertices of rhombic triacontahedron, truncated along the threefold axis. Choosing as a network of cluster centers TCC and decorating it by familiar 54-atom Mackay icosahedra (MI), the third shells can be added without conflicts around *half* of the MI. Heretofore, we shall call the MI with the third-shell *double* MI (DMI) (Ref. 18) (see Table I). In the TCC-based model, 96% of the atoms belong to the MI or the DMI. Throughout the paper, we will refer to the "connective" atoms in the model (i.e., to those not belonging to any of the perfectly icosahedral clusters) explicitly.

It is fair to point out that the quasiperiodicity of the

TCC remains a serious theoretical problem that has to be addressed in the future, but the available cubic approximants[19] have as much as about 2500 cluster centers,[20] or 1.8×10^5 atoms in the cubic unit cell, and are virtually indistinguishable from the true quasicrystal.

The outline of the paper is the following. In Sec. II we provide basic information about the TCC, which is described and analyzed elsewhere.[15] A technical description of the atomic decoration can be found in Sec. III. Instead of perfect alternation of the DMI and MI on the two kinds ("even" and "odd") of tiling nodes in the deterministic model, in Sec. IV we consider a modified model, in which the simple MI are fixed on all of the tiling nodes, but the deterministic rule forcing third icosahedral shells around half of the MI is replaced by a Monte Carlo algorithm maximizing the density of the remaining "connective" atoms. Finally, in Sec. V we compare calculated diffraction intensities of the deterministic model with the set of measured intensities.[5]

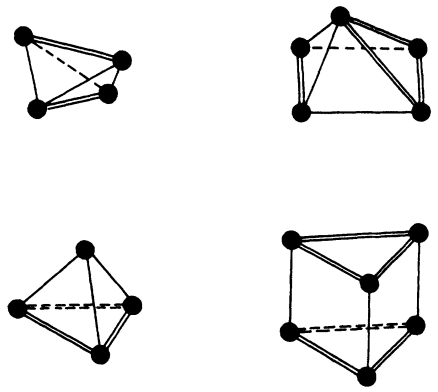

FIG. 1. *A* (top left), *B*, *C*, and *D* (bottom right) cells of the canonical tiling. *b* bonds (double lines) are decorated by RD, *c* bonds by PR. The interiors of *C* and *D* cells are filled by the additional PR (see Ref. 15) that are used in the description of atomic decoration.

II. TILING OF CANONICAL CELLS

It was soon recognized that the so-called 12-fold vertices (V_{12} theretofore) of the 3DPT are good candidates for the implementation of the cluster-based decoration, due to the icosahedral point symmetry of the 12 rhombohedral edges, pointing from the center to the 12 vertices of the icosahedron. The network of V_{12} is dominantly connected through twofold and threefold icosahedral bonds, called *b* and *c*, respectively. In terms of the familiar 3DPT building tiles (prolate rhombohedra, PR; oblate rhombohedra OE: it is convenient to consider also rhombic dodecahedra (RD), which is an assembly of two PR and two OR), the two bonds correspond to a long body diagonal of RD (*b* bond) and PR (*c* bond). Their lengths are $2.75a_q$ and $2.38a_q$, respectively, where a_q stands for the rhombohedron's edge length "quasilattice" parameter.

However, a small fraction of V_{12} in the 3DPT is linked through rhombohedron's edges and this connection is inconsistent with cluster-based decoration. After minimal removals, there remains about 91% of V_{12}, constituting true *bc* network of *b* and *c* bonds.[21]

The requirement of *maximal* density of the icosahedral *bc* network has led to the proposal of the tiling of four canonical cells (TCC).[15] The cells, called *A*, *B*, *C*, and *D* (Fig. 1), can be decorated by the RD, PR, and OR in such a way that the rhombohedra also tile the space. The nodes of the TCC become V_{12} of a rearranged rhombohedral tiling, but their density can be even *higher*, compared with the network of *all* V_{12} in the 3DPT, as suggested by transfer-matrix technique[22] and Monte Carlo optimization of density.[19]

Actually, while the density of rhombohedra is fixed by the "background" Goldstone mode strain, the density of TCC vertices *is not*. Eighteen *A* cells have the same volume as 4 *D* cells, but there are 3 tiling nodes per 18 *A* cells and only 2 nodes per 4 *D* cells (see Table II in Ref. [15]). At zero background Goldstone mode strain (quasiperiodic limit),

$$n_v=\tau^{-6}n_{\rm rh}(1+\epsilon)\ ,\quad n_A=6\tau^{-8}n_{\rm rh}(1+3\tau^2\epsilon)\ ,$$
$$n_{BC}=\tau^{-6}n_{\rm rh}\ ,\quad n_D=\tau^{-9}n_{\rm rh}(1-4\tau^3\epsilon)\ , \tag{1}$$

where $n_v, n_{\rm rh}, r, \ldots$ denote the densities of canonical ver-

TABLE I. TCC bonds and icosahedral clusters in the 6D representation. For bonds, *r* denotes their lengths, for cluster atoms, the distance from the center in the units of rhombohedrons edge a_q. For double MI, we list only shells additional to the simple MI. In the last column we list the positions of the corresponding atomic surface on 6D cubic lattice.

Name	6D vector	Mult.	*r*	6D position
b bond (RD)	(1,1,1,1,0,0)	30	2.753	
c bond (PR)	(1,1,1,0,0,0)	20	2.384	
		Simple MI		
Small icosahedron	$\frac{1}{2}$(1,0,0,0,0,0)	12	0.5	Edge
Icosidodecahedron	(1,0,0,0,0,0)	12	1.0	Node
	(1,−1,0,0,0,0)	30	1.052	Node
		Double MI		
20 triangles	(1,1,−1,0,0,0)	60	1.451	Node
τ-icos	$\frac{1}{2}$(1,1,1,1,1,1)	12	1.618	Body center

tices, rhombohedral vertices, and canonical cells, respectively. The parameter ϵ, measuring the deviation of the TCC to node density relatively to the density of V_{12} in the perfect 3DPT (equal to $\tau^{-6}n_{\rm rh}$), simplifies the arithmetic of Eq. (1) compared with the parameter $\zeta \equiv 9n_D/(9n_D+2n_A)$, defined in Ref. 15, though at the price of the loss of generality.[23] The case $\epsilon=0$ corresponds to the TCC ($\zeta=0.317$), in which local patterns of b and c bonds of the pure A, BC, and D tilings are forbidden.[15] The Monte Carlo study[16] suggests that ϵ might go up to $2\tau^{-9}$ in the quasiperiodic limit.

In an arbitrary TCC, the B and C cells are always paired: They adjoin either directly through the Y faces (equilateral triangles of b bonds) or through the D cell(s).[15] Throughout the paper, we shall treat the B-C pairs as a virtual BC cell.

III. DETERMINISTIC MODEL

Let us at first set up a few necessary conventions. The parity of a TCC node (or atom decorating TCC) at $\mathbf{r}=\sum_{i=1}^{6}n_i\mathbf{e}_i$ is even (odd), if $\sum_{i=1}^{6}n_i$ is even (odd), where we choose the six basis vectors e_i to point to the vertices of icosahedron in such a way that $\mathbf{e}_1$ is symmetrically surrounded by the remaining five basis vectors.[24] Lifting the TCC network from a three-space to a six-space is a standard procedure and was described in Ref. [15]. In this paper, we measure the distances in the units of "quasilattice parameter" a_q, the rhombohedron's edge length. In the i-Al-Mn-Si case, $a_q=4.6$ Å.

Our model is basically defined by the statement that 126-atom double-shell MI decorate even and 54-atom simple MI odd vertices of the tiling of canonical cells. The clusters involved in our model were described elsewhere[16,17] and their 6D representation is given in Table I. Except small distortions of some third-shell atoms along twofold directions that will be explained later, the clusters overlap and mutually share atoms along both twofold and threefold directions. The robust cluster decoration defined 96% of the atomic positions. In order to provide complete information about the model covering also atoms filling up the canonical interstitials, we have worked out a somewhat laborious labeling convention based on PR decorating TCC. A reader interested in technical details is recommended to consult also the original paper on TCC.[15]

Rhombohedral decoration of the TCC includes five kinds of PR: (1) PR(c), decorating c bonds: (2) PR(RD), constituting RD (two pairs of them are *overlapping* in the RD interior); (3) PR (BC), filling the BC-cell interior; (4) PR(Dc) in the D-cell interior along its threefold axis ("central"), and (5) PR(Da), three other PR in the D-cell interior, adjacent to the PR(Dc), and pointing to the three TCC vertices, which form equilateral triangles of b bonds. It is not necessary to consider OR; their atomic decoration is always determined by the adjacent PR, since the two OR (out of RD) in the rhombohedral decoration of the TCC never share face.

Let us consider PR with the vertices (000), (100) $+c.p.$, (110)$+c.p.$, and (111), where we choose first three of six icosahedral vectors as a basis ($\mathbf{e}_1\cdot\mathbf{e}_2=\mathbf{e}_1\cdot\mathbf{e}_3=\mathbf{e}_2\cdot\mathbf{e}_3=1/\sqrt{5}$). Now, since each PR is decorated symmetrically with respect to its threefold axis, we label each possible atomic position by a letter: tip, (000), denoted T; edges, $(1,0,0/2+c.p.,E;\tau^{-3}(1,1,1),N$ (projected from 6D nodes); τ^{-2} (1,1,1), G (projected from 6D body centers); and τ^{-1} (1,1,0), F (face diagonal point). Hence, the decoration of each PR can be described by the formula $\{T,E,N,G,F,F,G,N,E,T\}$, in which a minus sign will denote unoccupied orbit of sites and 1 or 3 occupied (with multiplicity 1 or 3); see Table II. We have omitted the remaining six PR vertices, because they are *always* occupied by atoms. One of the two possible decorations of PR(BC), which fits into the central hole of the triangle formed by RD decorating b bonds (called the Y face in Ref. 15), is shown on Fig. 2(b). In Fig. 2(c), the three PR(Da) in a D cell surround PR(Dc) (not shown). With respect to the Y face, the PR(Dc) is equivalent to PR(BC).

It is amusing to realize that the rhombic dodecahedra (RD) pack together in one of the two modes: "perpendicular," like in the α-Al-Mn-Si phase [see Fig. 2(a)], or "triangular," like in the β-Al-Mn-Si phase [see Fig. 2(b)] and Ref. 1. In TCC jargon, the first mode corresponds to the A cell and the second to the Y face. As a matter of fact, there are only very few atoms out of these two objects in the TCC model, which could explain the intriguing relationships between the i phase on the one hand and α and β phases on the other, suggesting that the i phase is an intermediate state between the α and β phases.[25]

TABLE II. Decoration of prolate rhombohedra. The notation is explained in the text. Parity ($+/-$) of each site is defined as a $\sum_{i=1}^{6}n_i$ (see Sec. III). The unoccupied "$T+$" sites are vacant DMI centers; unoccupied "$T-$" sites are vacant MI centers. Excepting PC(c), there are two ways of decorating each kind of PR, depending on the parity of its sharp-tip–cluster center. Atoms out of DMI and MI are marked by ($*$).

Name	$T+$	E	$N-$	$G+$	$F+$	$F-$	$G-$	$N+$	E	$T-$
PR(c)		3			3	3			3	
PR(RD)		3			3	3				1
PR(RD)	1			1		3	1		3	
PR(BC)		3			3	3		$*1$		$*1$
PR(BC)	$*1$			1		3			3	
PR(Dc)	$*1$			1		3				$*1$
PR(Dc)	$*1$		$*1$		$*3$		$*1$			$*1$
PR(Da)		3			3	3		$*1$		$*1$
PR(Da)	$*1$			1		3			3	

Modification of the RD decoration. Each twofold linkage between perfectly icosahedral DMI leads to short pair distances ($0.406a_q$) on the "top" and "bottom" faces of the RD decorating b bonds [see Fig. 2(b)]. In the Elser-Henley description of the α-phase structure,[1] the corresponding "Al(γ)" atoms are shifted from their "ideal" positions at the τ^{-1} and τ^{-2} points of the rhombohedron's face diagonal to the 1/3 and 2/3 face diagonal points. As explained elsewhere,[26] even more accurate modification of the α-Al-Mn-Si idealized structure is to distort only two pairs of atoms on the "top" and "bottom" faces of RD, linking two cluster centers. After this modification, the shortest pair distance in our model is $0.5a_q$ along fivefold directions in MI.

Density. In order to calculate how the atoms are apportioned among the cells, we at first associate them with TCC objects without sharing (for the sake of simplicity, the numbers per "even" and "odd" objects are averaged): nodes (54 MI atoms), b-bond "connective" atoms (five atoms in RD), BC-cell "connective" atoms [7/2 atoms of PR(BC)], and D-cell "connective" atoms [29/2 atoms in PR(Da) and PR(Dc)]. There are (1/6 MI + 1/2 RD) per A cell [1/2 MI + 3/2 RD + PR(BC)] per BC and [1/2 MI + 3/2 RD + 3 PR(Da) + PR(Dc)] per D cell. The result is shown in Table III and the compact expression for the total atom/Å^3 density of an arbitrary (period-

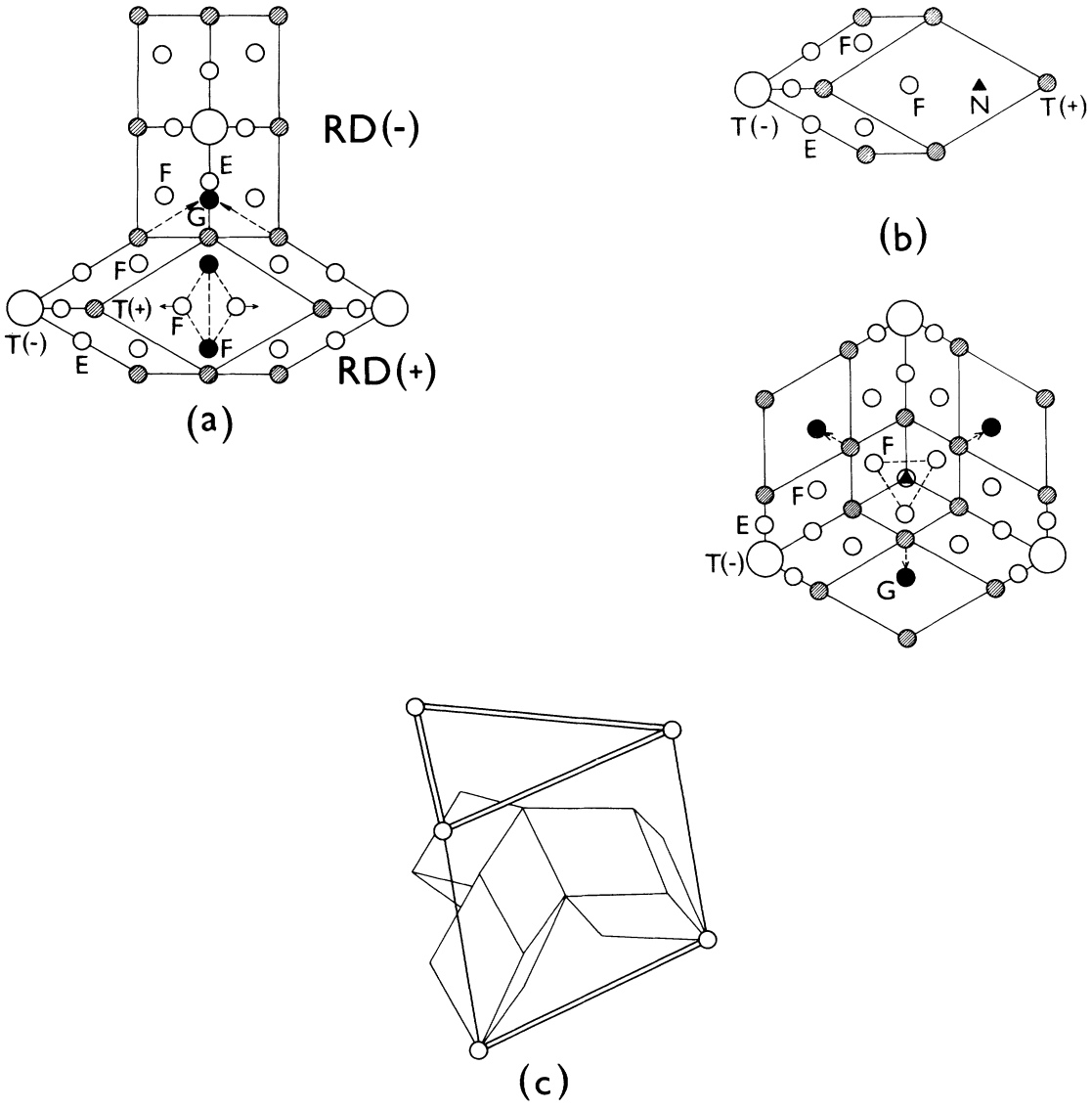

FIG. 2. Large open circles are centers of Mackay-icosahedra–vacant-TCC nodes. Small open circles are Al and dashed Mn atoms. Atoms are labeled by the convention explained in text. Solid circles are atoms located *under* rhombohedron's face and triangles denote atoms at the PR body diagonal. (a) Decoration of the A cell. Longer arrows point from even-parity MI centers (sharp RD tips) to the G atom [(Al(δ) via notation of Elser and Henley (Ref. 1)] in the interior of the adjacent odd-parity RD. Short arrows indicate that the pairs of F atoms, belonging to the third shell of DMI [they are called Al(γ) by Elser and Henley], are shifted to one- and two-thirds of the face diagonal, as proposed in Ref. 1. (b) Decoration of the Y face. Three RD packed in this mode form the hole in the center, into which PR(BC) is inserted. (c) Three PR(Da), decorating the D cell.

TABLE III. Atomic decoration of *A*, *BC*, and *D* cells. The atoms in the last column are included in column "others"; the numbers illustrate how a small fraction of atoms is not determined by the MI-DMI decoration rule.

	TCC-576	TCC-592	Node (MI)	*b* bond (RD)	Other	Sum	Out of MI, DMI
A	1320	1608	9	5/2		23/2	
BC	576	576	27	15/2	7/2	38	3/2
D	136	72	27	15/2	29/2	49	13/2

ic or quasiperiodic) model reads

$$\rho=\tfrac{1}{2}(23n_A+76n_{BC}+98n_D)\ . \tag{2}$$

Note that the 1/1 approximant (pure packing of *A* cells,[15] 12 *A* cells per unit cube) is exactly the α-Al-Mn-Si structure with 138 atoms per unit cube. Inserting $n_{\rm rh}=(\tau+2)^{3/2}/(2a_q^3\sqrt{5})$ into Eq. (1), where $a_q=4.6$ Å is the quasilattice constant, we find in the quasiperiodic limit the ($\epsilon=0$) density $\rho=0.0669$ atom/Å^3, or 3.611 g/cm^3 with the composition[27] $Al_{74.2}Mn_{20}Si_{5.8}$. In this model, about 4% of the atoms do not belong to MI or DMI.

Adjustability. The sensitivity of the physical properties to the variation of ϵ decreases as the homogeneity of the *A*-vs-*D* cell decoration increases. In the *i*-Al-Mn-Si model proposed here, *A* cells contain *only* MI or DMI atoms, but *D* cells certainly cannot be decorated equally densely; in the present model, we find 0.0680 at/Å^3 for *A*, 0.0670 for *BC*, and 0.0644 for the *D* cell. The ϵ variation can be quite impressive. Considering the known 8/5 TCC approximants,[19] 8% of the total volume can be decorated either by *A*- or *D*-cell-type structure; hence the density of the present model is adjustable in the interval 3.611–3.626 g/cm^3 with 4.2–3.1 % of the atoms out of MI or DMI.

6D fcc modulation. The perfectly icosahedral third shell around half of the TCC nodes leads to the atom-vacancy alternation that breaks the simple-cubic quasicrystal space group $P\bar{5}\bar{3}2/m$ into the face-centered $F\bar{5}\bar{3}2/m$. Although in the high-quality samples of *i*-Al-Mn-Si such ordering was not observed, there are more indications, justifying this approach: (i) Similar topological ordering is observed in *i*-Al-Cu-Fe and *i*-Al-Pd-Mn, which are structurally related phases; (ii) while in *i*-Al-Cu-Fe and *i*-Al-Pd-Mn the 6D fcc ordering is easily visible due to a robust *chemical* ordering, the atom-vacancy alternation in the *i*-Al-Mn-Si case leads only to a weak superlattice peak (see Sec. V); (iii) upon annealing and prior to the crystallization, the diffuse superlattice peaks develop in the diffraction pattern of *i*-Al-Mn;[28] (iv) the same atom-vacancy alternation is observed in the *a*-Al-Mn-Si phase.

6D atomic motifs. The model structure can be straightforwardly lifted to the 6D space, but since the acceptance domain of the quasiperiodic TCC is not known, in Fig. 3 we present the cuts through the 6D node and body-center atomic motifs of the 13/8 approximatant, based on random TCC tiling. There are four distinct atomic motifs: (1) Inner-shell MI sites are projected from the motifs at the edge midpoints of the 6D hypercubic lattice; the motif, not shown on Fig. 3, is a copy of the underlying TCC perpendicular-space image (2) "even" -node motif (3) "odd" -node motif, and (4) even-BC motif.

Comparison with 6D models. Both 6D and TCC models seek for the densest possible icosahedral network of 54-atom MI. There are two main differences and they seem to be mutually independent: (i) The density of the cluster-centers network is 10% higher in the TCC model, but so far we do not have a truly quasiperiodic solution to the tiling problem; (ii) while connective-atom ordering is 6D bcc in DO (Ref. 7) and Yamamoto's[8] models, in the TCC-based model it is 6D fcc. From a 6D point of view, a common feature of these models is an abrupt change of the real-space local environment when crossing the boundary of the cluster-center motif decorating 6D cubic lattice nodes, which is characteristic of models, consisting of strictly defined clusters and "connective" atoms. This feature is even more pronounced in the TCC model with perfectly icosahedral third shells.

Comparison with Yang's[17] *model.* Yang used two kinds of icosahedral clusters (MI and DMI) to build a quasiperiodic model of *i*-Al-Mn-Si. Instead of choosing a quasiperiodic network of cluster centers, he constructs an infinite hierarchical inflation procedure. The way the MI

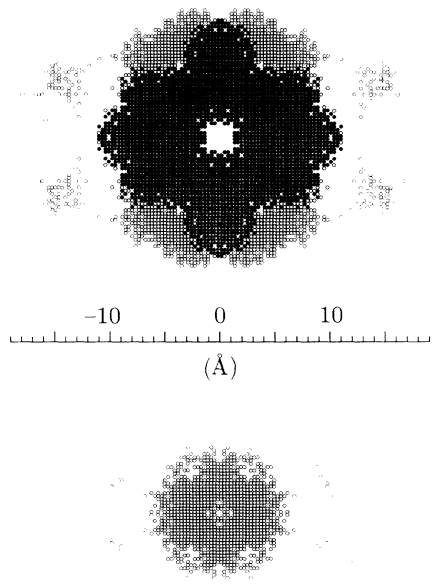

FIG. 3. 2D cut perpendicularly to the twofold axis through the node (top) and body-center motifs projected onto perpendicular space. The slice is 1.2 Å (four succeeding [100] planes) thick. The deterministic model, 13/8 approximant, has 185 252 atoms in the cubic cell ($\epsilon=0$); 96% of these atoms belong to 2440 icosahedral clusters. Larger circles correspond to even motif sites, smaller to odd; hence, the dark region is the identical part of both. Note that there is only "even" *BC* motif. Scale is in angstroms.

and DMI are linked (MI-DMI bonds along threefold, MI-MI and DMI-DMI bonds along twofold icosahedral directions) is an implicit definition of 6D fcc order. Since Yang forces quasiperiodicity of his model by a cluster-inflation algorithm with a vague definition of the filling of the gaps, it is not clear if the networks of the atoms and clusters can remain reasonably well connected after few inflation steps.

IV. PACKING EFFICIENCY AND 6D fcc ORDER

In this section we address the question, does the packing efficiency criterion play a role in the development of the 6D fcc order in *i*-Al-Mn-Si-type quasicrystals? We already know that constraining the minimum interatomic distance to $0.563a_q$, the densest packing obtained by the Monte Carlo density optimization is 6D sc structure, TCC with $\tau^{-3}b(0.649a_q)$ and $\tau^{-3}c(0.563a_q)$ bonds.[19] However, elsewhere[26] we have shown using the examples of 2/1, 3/2, and 5/3 cubic approximants of the *i*-Al-Mn-Si Monte Carlo model, that the 6D fcc-type structure is the maximal-density solution provided that the Mackay icosahedra, decorating nodes of the 12-fold packing network,[21] are *fixed* throughout the Monte Carlo annealing run.

The Monte Carlo version of the deterministic model of the 8/5 *i*-Al-Mn-Si approximant was designed as follows. At first, 54-atom Mi were fixed at each TCC node. Then we have generated third icosahedral shells (see Table I) from *both* even and odd TCC nodes and added all other reasonable connective-atom sites at the faces and body diagonals of PR decorating TCC, provided that they were not too close ($r>0.56a_q$) to the MI sites. Subsequently, the atoms were randomly created at these sites and allowed to jump to another close ($r<0.56a_q$) site, with the hard-core condition $r_{\min}>0.56a_q$ already switched on. The dynamics of the algorithm was significantly improved by forced $P2_13$ space symmetry: Each MC jump and/or creation of the atom was constrained to occur on the whole symmetry orbit at once. The whole MC run [(1) initialization MI at the TCC nodes, all third shell and other corrective-atom sites unoccupied; (2) MC connective-atom density maximization) was repeated many times and the densest solutions were recorded.

We have found that the density maximization actually *restored* third shells only around one kind (even or odd) of the TCC nodes, generating a model very similar to the deterministic one formulated in the previous section, with slightly higher atomic density (see Table IV). The cuts through the optimized domains were very similar to those already published[26] and to Fig. 3.

This result encourages us to conjecture that the 6D fcc modulation in *i*-Al-Mn-Si-type (*i*-Al-Pd-Mn, *i*-Al-Cu-Fe) quasicrystals is linked with the dominating stability of the 42-atom icosidodecahedron (its inner shell need not be Al icosahedra with a central vacancy such as in the *i*-Al-Mn-Si model; an alternative is partially occupied dodecahedron), playing a role of a building block in the quasiperiodic structure. Dense icosahedral packing of these units (TCC is the best candidate for such geometry, but 12-fold packing and similar networks also work) forces through a packing-efficiency requirement applied to "connective" atoms: (i) 6D fcc modulation, (ii) further maximization of local icosahedral symmetry (third icosahedral shells), and (iii) creation of (say) an even 6D body-center motif. It is natural to expect that the 6D fcc modulation of the atomic density (atom-vacancy alternation) should induce also some chemical modulation (atom-A-atom-B alternation), because two atoms with identical perpendicular position but different parity have in general different local environments. Obviously, also the appearance of the $0.618a_q$ pair distance from the 6D node to the 6D body-center site [(- 1 1 1 1 1 1)/2 in 6D notation] should contribute to the stability: (i) Environments of the 6D bc atoms are mostly perfectly icosahedral; (ii) this interatomic distance relaxes the strains that arise from the pure $\tau^{-3}b$ and $\tau^{-3}c$ bonding (which is favored by the packing-efficiency argument) with a c/b length ratio as large as $\sqrt{3}/2$.

V. DIFFRACTION

Calculated x-ray and neutron structure factors of the deterministic model in the 8/5 approximation were fitted to the experimental data.[5,29] Mn atoms were assigned to the vertices of the rhombohedral tiling, inscribed into the TCC (Ref. 15) (about 18% of the sites in the model) and to further 6D node-motif sites with the smallest magnitudes of perpendicular coordinate vectors—up to the $(AlSi)_{79}Mn_{21}$ composition.

We have minimized the residual R factor,

$$R=\left[\sum_{\mathbf{k}\neq 0}||F_c(\mathbf{k})|-F_o(\mathbf{k})|\right]\Big/\sum_{\mathbf{k}\neq 0}F_o(\mathbf{k})\ , \tag{3}$$

where F_o and F_c are observed and calculated structure factors,

$$F_c(|\mathbf{k}|)^2=\lambda^2\frac{1}{\mu^{\text{ico}}}\sum\mu_i^{\text{cub}}F_i^{\text{cub}}(|\mathbf{k}_i'|)^2\epsilon^{-Bk^2/2}\ . \tag{4}$$

In Eq. (4), μ^{ico} which stands for the total multiplicity of icosahedral orbits of reflections with the same $|\mathbf{k}|=[(N+M\tau)/(2+\tau)]^{1/2}/a_q$ (we used indexing after Ref. 30), scaling factor λ, and one global Debye-Waller (DW) temperature factor B are the parameters introduced into the minimization. All experimental x-ray and neutron icosahedral reflections have their cubic counter-

TABLE IV. 8/5 models ($\epsilon=0,576$ MI per cubic cell): the Monte Carlo (see Sec. IV) and deterministic. The density is expressed in atoms per rhombohedron vertex and "%" denotes the fraction of all atoms

Name	Atoms	MI (%)	*BC* motif (%)	Density	Space group	6D lattice
MC	43 880	70.9	4.8	4.245	$P2_13$	fcc
Deterministic	43 732	71.1	5.4	4.231	$P2_13$	fcc

parts with multiplicity $\mu^{\rm ico}=\sum\mu_i^{\rm cub}$, where i runs through all cubic orbits at $|\mathbf{k}_i'|$ on which an icosahedral orbit has been split.

We have obtained $R=0.089$ and 0.160 for x-ray and neutron data, respectively [Figs. 4(a,b)]. The Patterson functions along the fivefold axis calculated from the experimental and 8/5 model intensities (Fig. 5) also confirm the consistency of the two data sets. Especially the agreement between the neutron calculated and observed data with negative scattering length of the Mn is remarkable. We find only a weak R dependence on the following factors: global Goldstone mode (perpendicular-space) DW factor, ϵ variation of the initial canonical tiling [see Eq. (1)], and expansion or contraction of the first two MI shells, preserving their icosahedral symmetry[6] (though this modification in fact slightly decreased the neutron R factor to 0.141).

On the other hand, we find an obvious increase of both x-ray and neutron R factors, when a fraction of Al atoms on the 6D body-center positions is replaced by Mn, contrary to the conjecture that the 6D body-center motif is occupied by Mn.[7]

The 6D fcc modulation breaks the $Pa3$ space symmetry of the initial TCC to the $P2_13$.[31] As a consequence, in our perfectly ordered idealized model few odd-N reflections have detectable intensity [in Eq. (4) only the observed, even- N reflections are considered]. When the BC motif is occupied by Al, we find seven odd-N peaks with the intensity $I(\mathbf{k})>1\%$, the brightest of them (15/24, 47/76) approaching 3% of the 20/32 peak intensity.

We would like to note that our model is quite close to that proposed by Cahn and co-workers[5] (C model). A fraction of sites projected from the 6D body-center motif is 4.7 and 5.1% in the C and our model respectively, and the weights of the $Al(\alpha)$ motifs of the first MI shell atoms (these are in the C model assigned to the body-center motif) are 16.3 and 16.1%, corresponding to the relative number of MI units by about 10% higher than in the DO model. The similarity of the two models is, however, not surprising, since both of them closely follow the α-Al-Mn-Si phase structure.

Another comparison can be made with x-ray-absorption fine-structure (XAFS) experiments.[32] Ma and Stern concluded that cubic distortions of the MI units, observed in the i-phase and high MI-MI average coordination number (considering only the c-bond–PR connection between the clusters), $7.2\pm15\%$, imply the presence of α-phase microcrystallites in the i phase. Within the TCC framework it is very likely that distortions along twofold directions, equivalent or similar to the cubic distortions in the α phase, will be present also in the i phase. A fraction of the TCC nodes has locally (through b and c

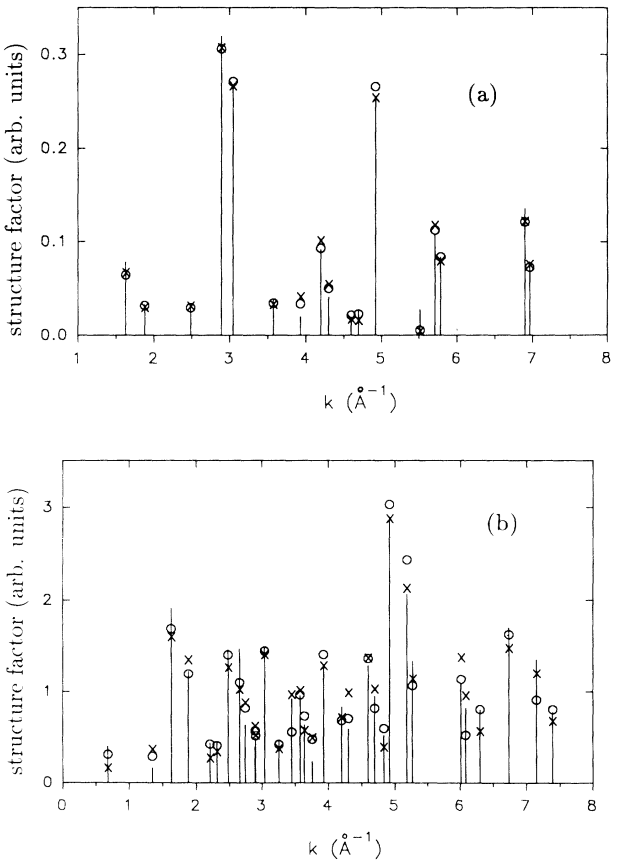

FIG. 4. X-ray (a) and neutron (b) structure factors. Bars are experimental data (Ref. 5), crosses calculated data, and open circles calculated data with expansion corrections (small Al icosahedron size 1.05, Mn icosahedron 1.03, Al icosidodecahedron 0.97) applied to MI atoms.

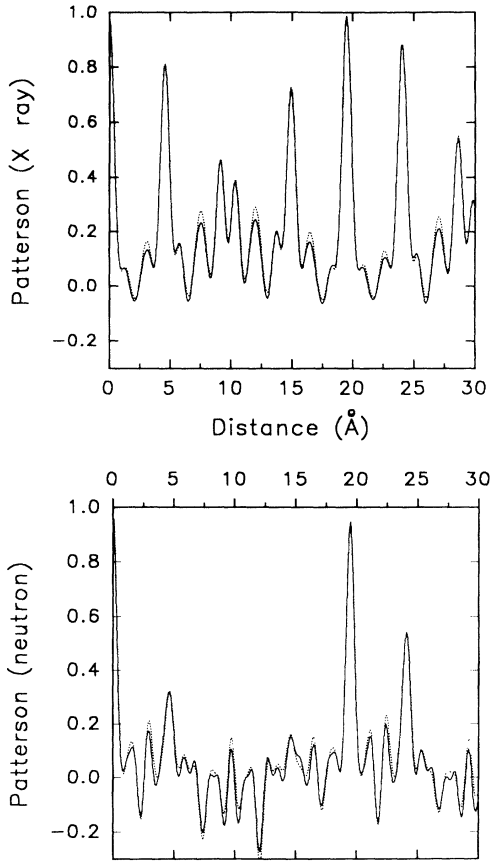

FIG. 5. X-ray (top) and neutron (bottom) Patterson function along the fivefold axis. The solid line is calculated from the experimental data, dotted line from the deterministic model.

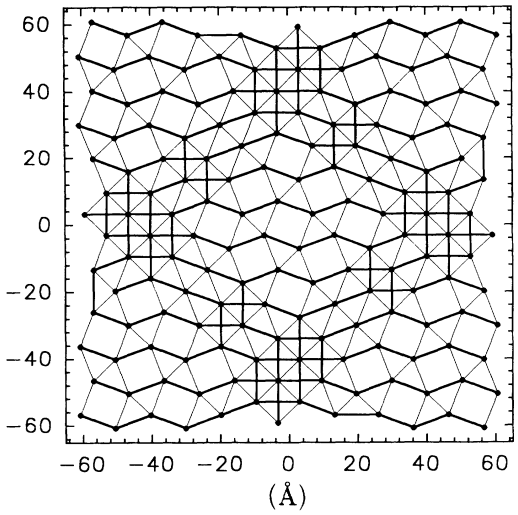

FIG. 6. Layer of 8/5 canonical tiling with 592 nodes per cubic cell. Thin lines are *b* bonds, thick lines *c* bonds. There are large fragments of the bcc structure.

bonds) identical environments with the α structure (the bcc structure fragments can be seen in the 8/5 TCC structure; see Fig. 6) and each *b* bond (linking MI in the icosahedral twofold directions) has in the present model one of two identical decorations (even, odd), inferred from the α phase. Furthermore, the densest 8/5 TCC approximant with 592 nodes per cubic cell investigated here has average MI-MI CN 6.66%, 7.5% below the experimental value, but clearly within the error bar (for comparison, the node in the 12-fold packing has about 5.6 *c* neighbors on average).

VI. CONCLUSION

We have proposed a deterministic tiling-decoration model of the *i*-Al-Mn-Si quasicrystal: Nodes of the tiling of four canonical cells (TCC) are occupied by a 54-atom MI, constituting the fundamental part of the structure. The density of MI units in our model exceeds by 10% their density in current 6D models.[7,8] Even-parity TCC nodes were decorated by additional, third icosahedral shells, observed in the α-Al-Mn-Si structure;[16] a MI with the third shell thus forms a 126-atom icosahedral cluster, called a double MI. Two remaining types of interstitials were filled by additional connective atoms. Since there are two kinds of nonequivalent icosahedral clusters, associated with even and odd TCC nodes, the space group of the quasiperiodic model is $F\bar{5}\,\bar{3}\,2/m$. The comparison of the calculated and experimental x-ray- and neutron-diffraction data gives *R* factors of 0.09 and 0.16, respectively.

The Monte Carlo version of the model with a MI fixed at the TCC nodes and densely ordered "connective" atoms confirmed that alternation of a DMI and a MI on the even and odd TCC nodes also provides the most efficient packing rule for the connective atoms (out of the MI). This result indicates, that 6D fcc order observed so pronouncedly in perfect quasicrystals with similar structure (*i*-Al-Pd-Mn,*i*-Al-Cu-Fe) can be linked with (i) stability of MI units (or their outer shells) and (ii) requirement of the most efficient (densest) packing of the connective atoms.

[1]V. Elser and C. L. Henley, Phys. Rev. Lett. **55**, 2883 (1985).
[2]P. Guyot and M. Audier, Philos. Mag. B **52**, L15 (1985).
[3]C. L. Henley and V. Elser, Philos. Mag. B **53**, L59 (1986).
[4]M. Audier and P. Guyot, in *Quasicrystals and Incommensurate Structures in Condensed Matter,* edited by M. J. Yacaman, D. Romeu, V. Castano, and A. Gomez (World Scientific, Singapore, 1990), p. 181.
[5]J. W. Cahn, D. Gratias, and B. Mozer, J. Phys. (Paris) **49**, 1225 (1988).
[6]M. De Boissieu, C. Janot, and J. M. Dubois, J. Phys. Condens. Matter **2**, 2499 (1990).
[7]M. Duneau and C. Oguey, J. Phys. (Paris) **50**, 135 (1989).
[8]A. Yamamoto, Phys. Rev. B **45**, 5217 (1992); in *Quasicrystals,* edited by T. Fujiwara and T. Ogawa (Springer-Verlag, Berlin, 1990), p. 57.
[9]M. Duneau and K. Katz, Phys. Rev. Lett. **54**, 2688 (1985).
[10]A. Katz, in *Number Theory and Physics,* edited by J. M. Luck, P. Moussa, M. Waldschmidt, and C. Itzykson (Springer-Verlag, Berlin, 1990), p. 100.
[11]M. Cornier-Quiquandon, A. Quivy, S. Lefebvre, E. Elkaim, C. Heger, A. Katz, and D. Gratias, Phys. Rev. B **44**, 2071 (1991).
[12]Z. Olami and S. Alexander, Phys. Rev. B **37**, 3973 (1988).
[13]A. P. Smith, J. Non-Cryst. Solids **153-154**, 258 (1993).
[14]M. Mihalkovič and P. Mrafko, J. Non-Cryst. Solids **156-158**, 936 (1993).
[15]C. L. Henley, Phys. Rev. B **43**, 993 (1991).
[16]H. A. Fowler, B. Mozer, and J. Sims, Phys. Rev. B **37**, 3906 (1988).
[17]Q. B. Yang, Philos. Mag. B **58**, 47 (1988).
[18]The name "double" MI was introduced by Yang. Contrary to the analysis of Fowler *et al.* (Ref. 16), Yang's DMI has an additional 30 atoms (altogether 156 in one DMI), decorating end points of the long rhombohedron's face diagonal (the distance from the cluster center at the other endpoint is $1.702a_q$). In this paper we actually borrow Yang's name for the cluster of Fowler *et al.* (without the last 30-atom shell). Although this last shell approximates the topological icosahedral order well, it is disordered *chemically.*
[19]M. Mihalkovič and P. Mrafko, Europhys. Lett. **21**, 463 (1993).
[20]Recently we have found a 34/21 approximant to the tiling of four canonical cells, containing 44 200 nodes in the cubic cell, so that one can hardly have a doubt about the existence of the quasiperiodic solution.
[21]C. L. Henley, Phys. Rev. B **34**, 797 (1986).
[22]M. Newman and C. L. Henley, J. Non-Cryst. Solids **153-154**, 205 (1993).
[23]It might not be quite clear, what is the value of the "3DPT" density of V_{12} in an *arbitrary* periodic rhombohedral tiling. In this paper we restrict ourselves to the cubic Fibonacci approximants; in that case (excepting 1/1 approximant) the "3DPT" density can be expressed in Fibonacci numbers.

[24]V. Elser, Acta Crystallogr. A **42**, 36 (1986).
[25]J.-M. Dubois and C. Janot, J. Phys. (Paris) **48**, 1981 (1988).
[26]M. Mihalkovič and P. Mrafko, J. Non-Cryst. Solids **143**, 225 (1992).
[27]M. Audier and P. Guyot, J. Phys. (Paris) Colloq. **47**, C3-405 (1986).
[28]N. K. Mukhopadhyay, S. Ranganathan, and K. Chattopadhyay, Philos. Mag. Lett. **60**, 207 (1989).
[29]D. Gratis, J. W. Cahn, and B. Mozer, Phys. Rev. B **38**, 1643 (1988).
[30]J. W. Cahn, D. Schechtman, and D. Gratias, J. Mater. Res. **1**, 13 (1986).
[31]It can be analytically shown that $Pa3 \rightarrow P2_13$ symmetry breaking in cubic approximants corresponds to 6D sc$\rightarrow$ 6D fcc symmetry breaking.
[32]Y. Ma and E. A. Stern, Phys. Rev. B **38**, 3754 (1988).

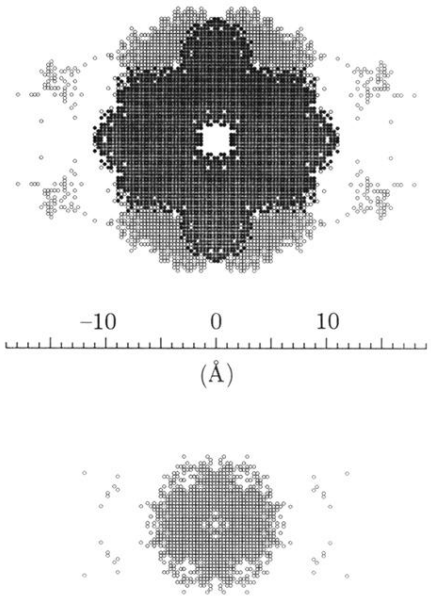

FIG. 3. 2D cut perpendicularly to the twofold axis through the node (top) and body-center motifs projected onto perpendicular space. The slice is 1.2 Å (four succeeding [100] planes) thick. The deterministic model, 13/8 approximant, has 185 252 atoms in the cubic cell ($\epsilon=0$); 96% of these atoms belong to 2440 icosahedral clusters. Larger circles correspond to even motif sites, smaller to odd; hence, the dark region is the identical part of both. Note that there is only "even" *BC* motif. Scale is in angstroms.